Acta Biochim Biophys Sin, 2015, 47(10), 842–850
doi: 10.1093/abbs/gmv081
Advance Access Publication Date: 7 September 2015
Original Article

Original Article

Distinct effects of Cu^{2+}-binding on oligomerization of human and rabbit prion proteins

Kejiang Lin[1], Ziyao Yu[1], Yuanhui Yu[2], Xinli Liao[2], Pei Huang[2], Chenyun Guo[2,*], and Donghai Lin[1,2,*]

[1]Department of Medicinal Chemistry, China Pharmaceutical University, Nanjing 21009, China, and [2]High-field NMR Research Center, College of Chemistry and Chemical Engineering, Xiamen University, Xiamen 361005, China

*Correspondence address. Tel/Fax: +86-592-2186078; E-mail: dhlin@xmu.edu.cn (D.L.)/guochy78@xmu.edu.cn (C.G.)

Received 22 April 2015; Accepted 12 June 2015

Abstract

The cellular prion protein (PrP^C) is a kind of cell-surface Cu^{2+}-binding glycoprotein. The oligomerization of PrP^C is highly related to transmissible spongiform encephalopathies (TSEs). Cu^{2+} plays a vital role in the oligomerization of PrP^C, and participates in the pathogenic process of TSE diseases. It is expected that Cu^{2+}-binding has different effects on the oligomerization of TSE-sensitive human PrP^C ($HuPrP^C$) and TSE-resistant rabbit PrP^C ($RaPrP^C$). However, the details of the distinct effects remain unclear. In the present study, we measured the interactions of Cu^{2+} with $HuPrP^C$ (91–230) and $RaPrP^C$ (91–228) by isothermal titration calorimetry, and compared the effects of Cu^{2+}-binding on the oligomerization of both PrPs. The measured dissociation constants (K_d) of Cu^{2+} were 11.1 ± 2.1 μM for $HuPrP^C$ and 21.1 ± 3.1 μM for $RaPrP^C$. Cu^{2+}-binding promoted the oligomerization of $HuPrP^C$ more significantly than that of $RaPrP^C$. The far-ultraviolet circular dichroism spectroscopy experiments showed that Cu^{2+}-binding induced more significant secondary structure change and increased more β-sheet content for $HuPrP^C$ compared with $RaPrP^C$. Moreover, the urea-induced unfolding transition experiments indicated that Cu^{2+}-binding decreased the conformational stability of $HuPrP^C$ more distinctly than that of $RaPrP^C$. These results suggest that $RaPrP^C$ possesses a low susceptibility to Cu^{2+}, potentially weakening the risk of Cu^{2+}-induced TSE diseases. Our work sheds light on the Cu^{2+}-promoted oligomerization of PrP^C, and may be helpful for further understanding the TSE-resistance of rabbits.

Key words: Cu^{2+}, prion oligomerization, affinity, conformational stability, TSE-resistance

Introduction

Prion proteins (PrPs) are cell-surface Cu^{2+}-binding glycoproteins that are responsible for prion diseases, the transmissible spongiform encephalopathies (TSEs) [1,2]. TSEs are fatal neurodegenerative diseases that are associated with the conversion of α-helix-rich cellular PrP (PrP^C) into β-sheet-rich scrapie form (PrP^{Sc}) [1,3–5]. The insoluble PrP^{Sc} has been treated as the pathogenic agent for many years. However, growing investigations suggest that the infectious prion is probably the soluble oligomer, the intermediate of the conformational transformation from PrP^C to PrP^{Sc} [6–8]. Thus, the oligomerization of PrP^C is believed to be a vital step in the pathogenic processes of prion diseases.

As an essential trace metal, copper plays fundamental roles in biological functions of the nervous system [9,10]. The central nervous system has high level of copper, and the brain comprises 2% of the total body mass but containing 7.3% of total body copper [11,12]. The imbalance of copper has been linked to neurodegenerative diseases, including prion diseases [13,14]. Increasing evidence supports the

participation of Cu^{2+} in the pathogenic processes of prion diseases [15–17]. Previous studies showed that Cu^{2+}-binding-induced protease resistance of PrP [18–21], and promoted conformational conversion of monomeric PrP^C into neurotoxic PrP oligomer [22]. At acidic condition, Cu^{2+} could promote the conversion of α-helical PrP^C into β-sheet oligomer with neurotoxicity. Furthermore, the Cu^{2+}-induced reactive oxygen species could also lead to conformational transition and aggregation of PrP [23]. Therefore, Cu^{2+}-binding plays a vital role in the oligomerization process of PrP^C.

Many mammals have been reported to be TSE-sensitive species with the potential of converting conformation of PrP from PrP^C to PrP^{Sc}, such as human, cattle, sheep, and mice [1,24–26]. On the contrary, rabbits are one of the few species that are resistant to prion diseases and have a low susceptibility to be infected by PrP^{Sc} [27]. Previous studies have suggested that the TSE-resistance of rabbit is mostly due to multiple amino acid residues in the rabbit PrP [27]. Although the protein misfolding cyclic amplification technique could be applied to overcome the species barrier in rabbit [28–30], rabbit is still one of the TSE-resistant species. Recent studies have demonstrated that the specific domains beyond PrP-H2H3 of rabbit remarkably affected the misfolding of rabbit PrP [31,32].

The resistance of rabbits to TSEs is highly associated with the difficulty of the conformational conversion of rabbit PrP^C ($RaPrP^C$) mostly due to the unique structural characteristics of $RaPrP^C$ [33,34]. The local structures of the copper-binding globular regions of $HuPrP^C$ and $RaPrP^C$ have been accessed by X-ray absorption fine structure technique and X-ray absorption near-edge structure technique [35,36]. The three-dimensional structures of copper-binding sites in $HuPrP^C$ (91–231) and $RaPrP^C$ (91–228) show substantial differences in both the coordination of amino acid residues and the copper bond. The copper bond in $RaPrP^C$ is longer than that in $HuPrP^C$, implying less Cu^{2+}-binding-induced conformational change of $RaPrP^C$ compared with that of $HuPrP^C$ [36]. It is thereby expected that Cu^{2+}-binding has distinctly different effects on the oligomerization of TSE-sensitive $HuPrP^C$ and TSE-resistant $RaPrP^C$. However, so far the distinct effects have not been addressed in detail. Obviously, the detailed roles played by Cu^{2+} in promoting oligomerization processes of both PrPs would be of great benefit to the understanding of the mechanism of TSE-resistance of rabbits.

In the present study, we measured the interaction of Cu^{2+} with $HuPrP^C$ and $RaPrP^C$ by isothermal titration calorimetry (ITC), and analyzed the Cu^{2+}-binding-promoted oligomerization of $HuPrP^C$ and $RaPrP^C$ by fast protein liquid chromatography (FPLC). We then compared the distinct effects of Cu^{2+}-binding on the secondary structures and conformational stabilities of $HuPrP^C$ and $RaPrP^C$ by circular dichroism (CD) spectroscopy.

Materials and Methods

Plasmid construction, protein expression, and purification

The gene fragment encoding either $HuPrP^C$ (91–230) or $RaPrP^C$ (91–228) was inserted into the vector pET-30a via *Nde*I and *Xho*I restriction sites and then transformed into *Escherichia coli* BL21(DE3) strain. The cells were cultured in 2× YT medium containing 0.05 mg/ml kanamycin at 37°C. When the $A_{600\ nm}$ reached between 0.8 and 1.0, 1.0 mM isopropyl-β-D-thiogalactoside was added and cells were grown for another 4 h. Then, cells were harvested by centrifugation at 9000 rpm for 4 min at 4°C, and re-suspended in the buffer (20 mM Tris, 2 mM EDTA, 150 mM NaCl, 100 μg/ml lysozyme, 0.1% Triton X-100, 1 mM PMSF, pH 7.4), followed by sonication for 30 min. After centrifugation at 11,000 rpm for 25 min at 4°C, the inclusion bodies were collected and washed with the buffer (20 mM Tris, 150 mM NaCl, 0.5% Triton X-100, 2 M NaCl, 4 M urea, pH 7.4). The resulting pellets were dissolved in the buffer (10 mM Tris, 100 mM Na_2HPO_4, 0.5% Triton X-100, 10 mM β-Mercaptoethanol, 6 M GdnHCl, pH 8.0) and refolded by dialysis using the buffer (10 mM Tris, 100 mM Na_2HPO_4, pH 8.0) with a linear gradient 6–0 M GdnHCl. The resulting protein solution was purified by FPLC on a 10/300 Superdex 75 column (GE Healthcare, Wisconsin, USA) with the elution buffer (20 mM NaOAc, 0.02% NaN_3, pH 5.5). The protein purity was assessed by 15% sodium dodecyl sulfate–polyacrylamide gel electrophoresis. The purified protein solution was concentrated by ultracentrifugation and the protein concentration was determined using NanoVue plus (GE Healthcare) at 280 nm with the extinction coefficient of $22 \times 10^3\ M^{-1}\ cm^{-1}$ calculated from the amino acid sequences of $HuPrP^C$ (91–230) and $RaPrP^C$ (91–228) by the web-based tool provided by ExPasy.

Size exclusion chromatography

Size exclusion chromatography was performed using ÄKTA FPLC equipment (GE Healthcare). Five column volumes of elution buffer were used to equilibrate the column prior to the experiments. The flow rate was 0.4 ml/min and the protein elution was monitored by ultraviolet absorption at 280 nm.

Oligomeric prion preparation

The purified $HuPrP^C$ (91–230) and $RaPrP^C$ (91–228) proteins were diluted to 40 μM in the buffer (20 mM NaOAc, 150 mM NaCl, 0.02% NaN_3, pH 4.0). The samples were kept in the thermostatic water bath at 37 and 42°C for 80 min without or with 40–480 μM of $Cu(OAc)_2$, respectively. Products were further separated by 10/300 Superdex 75 column (GE Healthcare) for the subsequent experiments. Data were processed with the software Unicorn 5.2.

Isothermal titration calorimetry

The dissociation constant (K_d) and stoichiometry (N) of the interaction between Cu^{2+} and PrP^C was measured by ITC using an ITC200 calorimeter (GE Healthcare). Calorimetric titration of Cu^{2+} to PrP^C was performed at 25°C in acetate buffer (20 mM NaOAc, pH 5.5). Time between injections was 150 s. ITC data were analyzed by integrating the heat effects after the data were normalized to the amount of injected protein. Data fitting was conducted to determine the dissociation constant and stoichiometry based on a single-site binding model using the Origin software package (GE Healthcare).

CD spectroscopy

All CD spectra were recorded on a Jasco J-810 spectropolarimeter (Jasco, Tokyo, Japan) interfaced with a Peltier-type temperature control at 25°C. The reported spectra were an average of three consecutive scans and blanked with respective buffers. Far-UV CD spectra were collected in the wavelength range of 200–250 nm using 1-mm path length. The spectra were recorded in continuous scanning mode at a scanning rate of 50 nm/min with a step size of 0.2 nm and a bandwidth of 1 nm. To conduct urea-induced unfolding transition experiments, the range of urea concentrations up to 10 M was used with 0.5 M gradient. The $Cu(OAc)_2$ stock solution was added into the protein solution prior to titrating the stock solution of urea.

Results

Cu^{2+} bound to PrP^C with moderate affinity

For the experiments of metal binding to PrP, it is very important that the protein should be in its apo state. We thus measured the metal content by using inductively coupled plasma mass spectrometry. Our results showed that the protein samples did not contain any metal atoms and were indeed in the apo state (data not shown).

The thermodynamic parameters of equilibrium interaction between protein and ligand can be accurately determined by ITC [37]. ITC experiments were carried out to measure the interactions of Cu^{2+} with $HuPrP^C$ (91–230) and $RaPrP^C$ (91–228) at pH 5.5 (**Fig. 1** and **Table 1**). The Cu^{2+} titration yielded positive heat deflection in the ITC curve, indicating that the Cu^{2+} titration progress was associated with the endothermic reaction (**Fig. 1**). Both $HuPrP^C$ (91–230) and $RaPrP^C$ (91–228) bound Cu^{2+} with a binding stoichiometry (N) close to 1, suggesting that one PrP^C molecule bound one Cu^{2+} molecule (**Table 1**). The results derived from the ITC curves showed that Cu^{2+} had moderate affinities for both proteins at mild acidic condition (pH 5.5). The dissociation constant (K_d) of $HuPrP^C$–Cu^{2+} interaction was 11.1 ± 2.1 μM, while that of $RaPrP^C$–Cu^{2+} was 21.1 ± 3.1 μM, indicating that $HuPrP^C$ bound Cu^{2+} with an affinity higher than $RaPrP^C$.

To confirm that the proteins remained monomeric during ITC experiments with very rapid stirring, size exclusion chromatography was used to analyze the protein samples. The results showed that the proteins did remain monomeric (**Supplementary Fig. S1**), indicating that both $HuPrP^C$ (91–230) and $RaPrP^C$ (91–228) did not aggregate during the ITC experiments.

Cu^{2+}-binding promoted the oligomerization of PrP^C

The size exclusion chromatography was applied to analyze the percentages of PrP^C monomers and oligomeric PrP (PrP^O) oligomers. The peaks around 7 and 13 ml represented the oligomeric PrP^O and monomeric PrP^C, respectively (**Fig. 2A,B**). In the absence of Cu^{2+}, the oligomerization was observed in acidic buffer (20 mM NaOAc, 150 mM NaCl, 0.02% NaN_3, pH 4.0). The percentages of $HuPrP^O$ and $RaPrP^O$ were 62.2% and 23.8%, respectively. This result illustrated that more $HuPrP^O$ proteins were formed compared with $RaPrP^O$ proteins. Expectedly, in the presence of Cu^{2+}, the percentage of monomer was decreased significantly whereas the percentage of oligomer was increased markedly (**Fig. 2A,B**), indicating that Cu^{2+}-binding significantly promoted the oligomerization of PrP^C. Moreover, the oligomerization of PrP^C was dependent on the Cu^{2+} concentration (**Fig. 2C**). After incubation with 1 molar equivalent (eq.) of Cu^{2+} (40 μM) at 42°C, the $HuPrP^O$ percentage was 81.9% with an increase of 19.7%, while the $RaPrP^O$ percentage was 32.6% with an increase of 8.8% only (**Fig. 2C**). Furthermore, when incubated with 12 eq. of Cu^{2+}, the $HuPrP^O$ percentage was increased by 29.2%, whereas the $RaPrP^O$ percentage was increased by only 24.8%. These results showed that Cu^{2+}-binding promoted the oligomerization of $HuPrP^C$ more significantly than that of $RaPrP^C$ at 42°C.

Table 1. Binding parameters derived from the ITC curves of monomeric $HuPrP^C$ (91–230) and $RaPrP^C$ (91–228) titrated with Cu^{2+}

PrP^C	n	K_d (μM)	ΔH (cal/mol)	ΔS (cal/mol/deg)
$HuPrP^C$ (91–230)	1.07 ± 0.02	11.1 ± 2.1	3833 ± 95.0	35.6
$RaPrP^C$ (91–228)	0.99 ± 0.02	21.1 ± 3.1	4180 ± 95.4	35.4

The ITC experiments were performed at 25°C with acetate buffer (20 mM NaOAc, pH 5.5). The concentrations of $HuPrP^C$ (91–230), $RaPrP^C$ (91–228), and Cu^{2+} are 0.4, 0.4, and 4.5 mM, respectively.

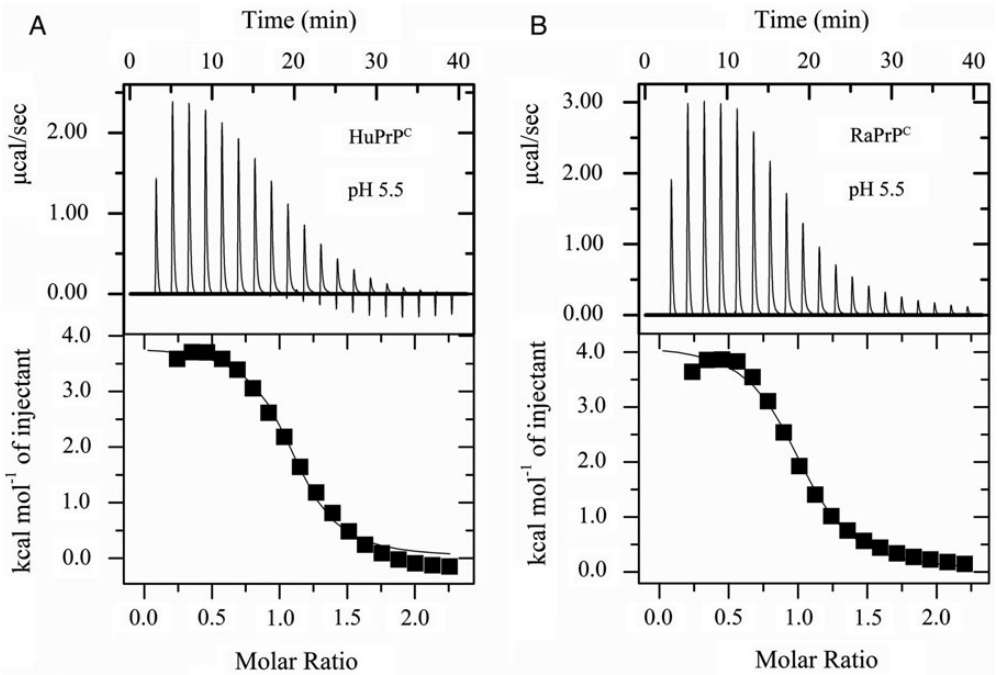

Figure 1. Ligand-binding assays of monomeric $HuPrP^C$ (91–230) and $RaPrP^C$ (91–228) with Cu^{2+} by ITC The representative raw ITC data and the fitted binding curves are shown for the proteins $HuPrP^C$ (A) and $RaPrP^C$ (B). The ITC experiments were performed at 25°C with acetate buffer (20 mM NaOAc, pH 5.5). The concentrations of $HuPrP^C$ (91–230), $RaPrP^C$ (91–228), and Cu^{2+} are 0.4, 0.4, and 4.5 mM, respectively.

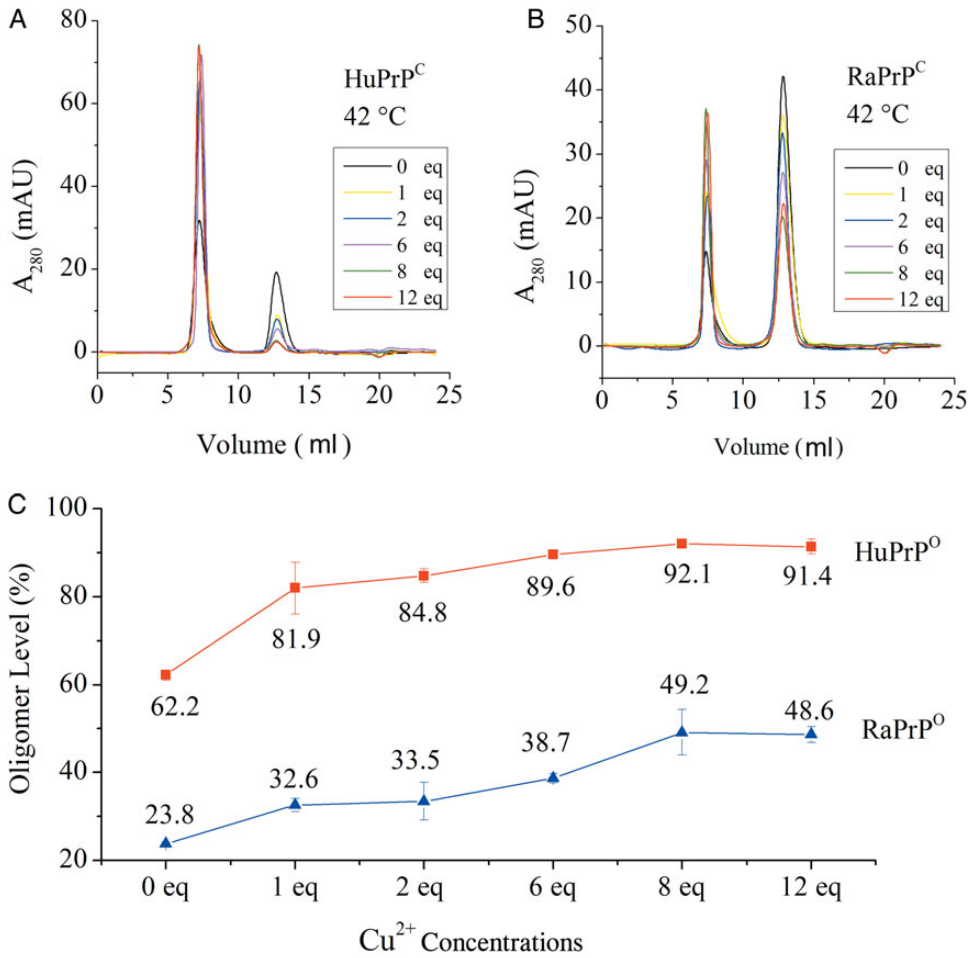

Figure 2. Oligomerization of $HuPrP^C$ (91–230) and $RaPrP^C$ (91–228) with different concentrations of Cu^{2+} (A,B) Size exclusion chromatography profiles of the oligomerization of $HuPrP^C$ and $RaPrP^C$ with 0–12 eq. of Cu^{2+}. (C) The oligomer levels of $HuPrP^O$ and $RaPrP^O$ formed with 0–12 eq. of Cu^{2+}. The PrP^O oligomers were formed at 42°C in the buffer (20 mM NaOAc, 150 mM NaCl, pH 4.0).

Monomeric PrP^C and oligomeric PrP^O adopted different conformations

CD spectroscopy was applied to compare the secondary structures of monomeric and oligomeric PrPs (**Supplementary Fig. S2**). The CD spectra indicated that both $HuPrP^C$ and $RaPrP^C$ adopted typical α-helical structures with well-defined negative peaks at 208 and 222 nm. However, the CD spectra showed one negative peak at 217 nm for $HuPrP^O$ and $RaPrP^O$ prepared either in the presence or in the absence of Cu^{2+}, indicating that both $HuPrP^O$ and $RaPrP^O$ adopted β-sheet-rich structures. These results show the distinct difference of conformation between the monomeric PrP^C and oligomeric PrP^O.

Cu^{2+}-binding changed the secondary structure of PrP^C

CD experiments were conducted at 25°C to measure the Cu^{2+}-binding-induced changes in secondary structures of both $HuPrP^C$ (91–230) and $RaPrP^C$ (91–228) in acetate buffer (20 mM NaOAc, pH 5.5). The oligomerization of PrP^C was negligible at such a low temperature (data not shown). In the absence of Cu^{2+}, the far-UV CD spectra showed two negative peaks at 208 and 222 nm, indicating that both $HuPrP^C$ and $RaPrP^C$ adopted α-helix-rich structures (**Fig. 3**). When 1 eq. of Cu^{2+} was added, the CD spectrum of $HuPrP^C$ began to shift up (**Fig. 3A**), whereas that of $RaPrP^C$ had a small shifting-down (**Fig. 3B**). With the addition of Cu^{2+} up to 4 eq., the CD spectra of $HuPrP^C$ shifted more significantly than those of $RaPrP^C$. In the presence of 8–16 eq. of Cu^{2+}, the CD spectra gradually became one negative peak at 217 nm, implying the generation of β-sheet-rich structure (**Fig. 3A**, right). Compared with those of $HuPrP^C$, the CD spectra of $RaPrP^C$ shifted up more slowly, although the characteristic of β-sheet-rich structure was observed with the addition of Cu^{2+} up to 16 eq. (**Fig. 3B**, right). Furthermore, the CD spectra of $RaPrP^C$ did not reach a roughly stable level-like $HuPrP^C$ even with the addition of 16 eq. of Cu^{2+} (**Fig. 3B**, right). These results indicated that Cu^{2+}-binding can significantly change the secondary structures of both $HuPrP^C$ and $RaPrP^C$, and induce the conformational conversion of PrP^C from α-helix-rich structure to β-sheet-rich structure. The Cu^{2+}-binding-induced secondary structural change of $HuPrP^C$ is more remarkable than that of $RaPrP^C$.

Cu^{2+}-binding decreased the conformational stability of PrP^C

To address the effects of Cu^{2+} on the conformational stabilities of $HuPrP^C$ and $RaPrP^C$, urea-induced unfolding transition experiments were performed by far-UV CD spectroscopy (**Fig. 4**). Both $HuPrP^C$ and $RaPrP^C$ completely lost their secondary structures in the presence

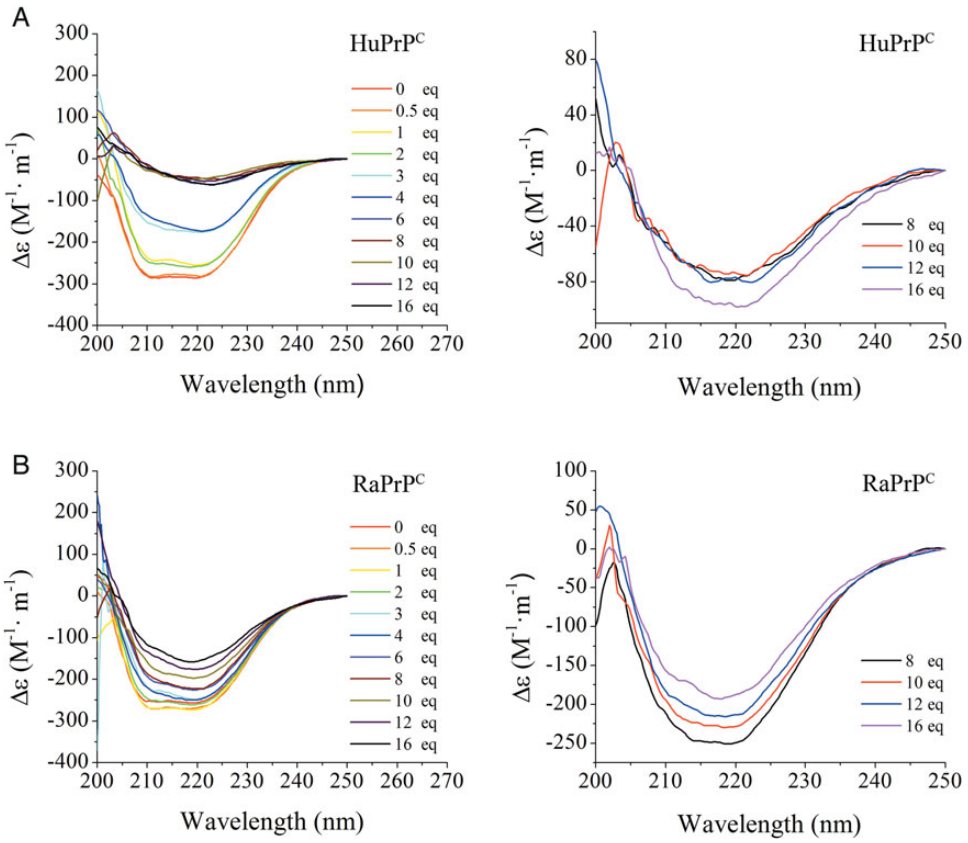

Figure 3. Far-UV CD spectra of $HuPrP^C$ (91–230) (A) and $RaPrP^C$ (91–228) (B) titrated by different concentrations of Cu^{2+} The CD experiments were performed at 25°C with acetate buffer (20 mM NaOAc, pH 5.5). The concentrations of Cu^{2+} are from 0 to 160 μM.

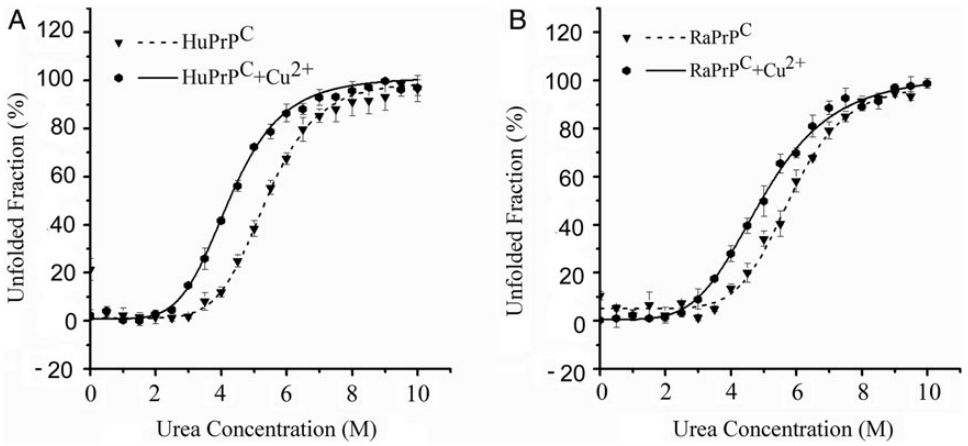

Figure 4. Effects of Cu^{2+} on the urea-induced unfolding transitions of monomeric $HuPrP^C$ (91–230) (A) and $RaPrP^C$ (91–228) (B) The CD experiments were performed at 25°C with acetate buffer (20 mM NaOAc, pH 5.5). The concentrations of $HuPrP^C$ (91–230), $RaPrP^C$ (91–228), and Cu^{2+} are 10 μM, respectively.

of 10 M urea. The apparent thermodynamic parameters of urea-induced unfolding transition for rabbit PrP^C and its variants were described previously [33,34]. C_m is the concentration of urea required to denature 50% of a protein, and $\Delta G^{H_2O}_{N\rightarrow U}$ represents the apparent estimated free energy change of unfolding extrapolated to zero concentration of denaturant.

In the absence of Cu^{2+}, the measured C_m values of $HuPrP^C$ and $RaPrP^C$ were 5.37 ± 0.07 and 5.83 ± 0.09 M, respectively (Table 2), indicating that the conformational stability of $HuPrP^C$ was lower than that of $RaPrP^C$. In the presence of Cu^{2+}, the C_m values of $HuPrP^C$ and $RaPrP^C$ were 4.27 ± 0.04 and 4.98 ± 0.07 M, respectively. Cu^{2+}-binding decreased the C_m values of $HuPrP^C$ and $RaPrP^C$ by

Table 2. Apparent thermodynamic parameters of urea-induced unfolding of monomeric $HuPrP^C$ (91–230) and $RaPrP^C$ (91–228) in the presence and absence of Cu^{2+}

	$\Delta G_{N\to U}^{H_2O}$ (kJ/mol)		$m_{N\to U}$ (kJ/mol/M)		C_m (M)	
Cu^{2+}	−	+	−	+	−	+
$HuPrP^C$	13.35 ± 0.85	12.77 ± 1.45	−2.34 ± 0.14	−2.59 ± 0.15	5.37 ± 0.07	4.27 ± 0.04
$RaPrP^C$	14.91 ± 0.88	13.20 ± 0.52	−2.73 ± 0.16	−2.46 ± 0.09	5.83 ± 0.09	4.98 ± 0.07

The CD experiments were conducted with acetate buffer (20 mM NaOAc, pH 5.5) at 25°C. $\Delta G_{N\to U}^{H_2O}$ is designated as the apparent free energy change of unfolding extrapolated to zero concentration of denaturant, $m_{N\to U}$ is the cooperativity of the unfolding transition, and C_m is the concentration of urea required to denature 50% of the protein. The concentrations of $HuPrP^C$ (91–230), $RaPrP^C$ (91–228), and Cu^{2+} are 10 μM, respectively.

~1.1 and 0.9 M, respectively. These results indicated that the conformation of $HuPrP^C$ is less stable than that of $RaPrP^C$, and Cu^{2+}-binding decreases the conformational stability of $HuPrP^C$ more significantly than that of $RaPrP^C$.

Discussion

Previous studies have demonstrated that the central nervous system has high level of copper [11,12] and copper plays crucial roles in TSE diseases [38–41]. However, the underlying mechanisms of Cu^{2+} participating in the pathogenic processes of prion diseases have not been well addressed. Recently, Wu *et al.* [22] demonstrated that Cu^{2+} could promote the formation of neurotoxic PrP oligomer and play a vital role in the oligomerization of PrP^C. Their work showed that Cu^{2+} could promote α-helical $HuPrP^C$ (91–230) converting to soluble β-sheet oligomer at acidic environment (pH 5.0), and the Cu^{2+}-induced oligomer generated significant damage in human SK-N-SH neuroblastoma cells. However, the details of Cu^{2+}-induced oligomerization process of PrP^C remain unclear. It is expected that Cu^{2+} regulates the pathogenic processes of prion diseases via participating in the oligomerization process of PrP^C. Thus, exploring the relationship between Cu^{2+} and the oligomerization of PrP^C could be helpful for the mechanistic understanding of prion diseases. Previous work showed that human beings are susceptible to TSE diseases, but rabbits are resistant to TSE diseases. It could be speculated that Cu^{2+}-binding promoted oligomerization of PrP differently between TSE-sensitive $HuPrP^C$ and TSE-resistant $RaPrP^C$. In the present study, we confirmed that Cu^{2+}-binding induces conformational transformation of PrP^C [22,42–44], and promotes the oligomerization of PrP^C [22]. More importantly, our results also demonstrated that Cu^{2+}-binding promotes the oligomerization of $HuPrP^C$ more significantly than that of $RaPrP^C$ (**Fig. 2**).

ITC experiments under acidic condition were conducted to mimic the environment in the endosomal–lysosomal system which is related to the pathogenesis of prion diseases [45]. The results showed that Cu^{2+} bound to $HuPrP^C$ (91–230) and $RaPrP^C$ (91–228) with moderate affinities (10^5 M^{-1}) at pH 5.5. However, a previous study showed that Cu^{2+} bound to mouse PrP^C (91–231) with 10-fold higher affinity (10^6 M^{-1}) at pH 6.6 [46]. Nevertheless, this study also showed that the affinity of Cu^{2+} with PrP^C was pH-dependent, and low pH could decrease the affinity of Cu^{2+} with PrP^C [46]. The affinity difference between our study and the previous study might be mostly due to the different pH conditions used.

Furthermore, our ITC data showed that the affinity of $HuPrP^C$ (91–230) for Cu^{2+} is higher than that of $RaPrP^C$ (91–228) (**Table 1**). It could thus be speculated that $HuPrP^C$ (91–230) potentially underwent more significant conformational change than $RaPrP^C$ (91–228) due to Cu^{2+}-binding (**Fig. 3**). Previous works indicated that Cu^{2+} mainly binds to the amyloid fragment of PrP^C containing the residues His 95/96, His 110/111, and Met 108/109 [35,36]. It has been suggested that the flexible region might make significant contribution to the misfolding of PrP and forming toxic agent [47–49]. Cu^{2+} binding to PrP^C would induce significant change in the spatial structure of this region and thereby promote the oligomerization of PrP^C.

Jones *et al.* [50] found that Cu^{2+}-binding to His-96 and His-111 resulted in an increase in β-sheet, which coupled with a loss of irregular structure in this fragment (residues 90–126) in PrP^C. Our CD results indicated that Cu^{2+}-binding promoted the conformational conversion of PrP^C from α-helix-rich structure to β-sheet-rich structure at mild acidic environment (pH 5.5; **Fig. 3**). Younan *et al.* [43] found that Cu^{2+}-binding could lead to the loss of α-helical structures but could not induce the increase in β-sheet content of PrP (23–231) at neutral environment (pH 7.4). These results may suggest that acidic environment facilitates Cu^{2+}-binding-induced conformational change in PrP^C [22].

The ITC data indicated that Cu^{2+} bound to $HuPrP^C$ (91–230) and $RaPrP^C$ (91–228) with moderate affinities (**Table 1**). The thermodynamic parameter derived from an ITC experiment includes contributions from all the events that might occur in the molecules going from free to bound state [51], such as the protein structural change. Therefore, it is possible that our ITC results also include certain contributions made by some protein structural changes. Furthermore, no significant secondary structure change was detected in far-UV CD experiments when 1 eq. of Cu^{2+} was added to either $HuPrP^C$ or $RaPrP^C$ (**Fig. 3**). However, Cu^{2+}-binding-induced conformational conversion of PrP^C from α-helix-rich structure to β-sheet-rich structure was obviously observed when 8 eq. of Cu^{2+} was added (**Fig. 3**). The ITC data showed that the affinity of Cu^{2+} for $HuPrP^C$ was higher than $RaPrP^C$, probably explaining the observation that CD spectra of $HuPrP^C$ changed more significantly than those of $RaPrP^C$ when Cu^{2+} was titrated to the PrP^C solutions (**Fig. 3**). These results showed that $HuPrP^C$ is more readily to change its conformation upon Cu^{2+}-binding compared with $RaPrP^C$. In other words, $HuPrP^C$ is more susceptible to Cu^{2+}-binding than $RaPrP^C$.

The urea-induced unfolding transition experiments demonstrated that Cu^{2+}-binding decreased the conformational stabilities of $HuPrP^C$ and $RaPrP^C$ (**Fig. 4**), which might be due to the secondary structure changes induced by Cu^{2+}-binding. Previous work demonstrated that Cu^{2+}-binding-induced protein destabilization could facilitate the conformational conversion and oligomerization of PrP^C [20,52]. In the presence of Cu^{2+}, the conformational stability of $HuPrP^C$ decreased more significantly than that of $RaPrP^C$ (**Table 2**). These results might explain the observation that the percentage of $HuPrP^O$ was increased more significantly in the presence of Cu^{2+} than that of the $RaPrP^O$ (**Fig. 2**).

In addition, we explored the conformational stabilities of oligomeric PrP^O in the presence or in the absence of Cu^{2+} by urea-induced unfolding transition experiments (**Supplementary Fig. S3 and Table S1**). The measured C_m values of $HuPrP^O$ with and without Cu^{2+} were 6.28

± 0.25, and 4.37 ± 0.12 M, respectively. Those values of $RaPrP^O$ with and without Cu^{2+} were 5.03 ± 0.14 and 4.33 ± 0.08 M, respectively. In the present study, the thermal-induced PrP^O without Cu^{2+} was found to be less stable than PrP^C. However, previous studies showed that the denaturant-induced β-rich isoform of PrP was thermodynamically more stable than the native PrP [53,54], which contradicted our results of this work. We think that the contradiction was resulted from different experimental conditions. The oligomers formed under different experimental conditions (pH, salt concentration, and denaturant) were pleomorphic [7,55–57], and could have somewhat different properties and possess different stabilities. In the previous studies, the prion oligomers were prepared in several days with denaturants (either urea or GdnHCl) under acidic conditions at room temperature (23°C). In the present study, oligomers were prepared by incubating proteins in the buffer without denaturants at 42°C, and obtained in much shorter time (80 min). It is expected that the stability of denaturant-induced oligomers is somewhat different from that of thermal-induced oligomers, and the status of denaturant-induced oligomers might be more similar to that of PrP^{Sc} which is more stable than PrP^C. Moreover, different buffers were used for the equilibrium denaturation of PrP in the previous studies and our study. In this study, we used the buffer without NaCl (20 mM NaOAc, pH 5.5) in urea-induced unfolding transition experiments, which could significantly reduce the thermodynamic stability of PrP^C [58], while in the previous studies, authors used the buffer with NaCl (20 mM NaOAc, 0.2 M NaCl, pH 3.6) [54]. In the absence of Cu^{2+}, $HuPrP^O$ possesses similar conformational stability to $RaPrP^O$. However, in the presence of Cu^{2+}, $HuPrP^O$ possesses significantly higher conformational stability than $RaPrP^O$. These results showed that Cu^{2+} could enhance the conformational stability of PrP^O, and Cu^{2+} enhanced the conformational stability of $HuPrP^O$ more significantly than that of $RaPrP^O$. However, the underlying mechanisms have not been addressed. Studies on the interaction of Cu^{2+} with other misfolded proteins that are highly associated with neurodegenerative disorders will provide a better understanding of the conformational stability of PrP^O enhanced by Cu^{2+}. As well known, amyloid-β (Aβ) is responsible for Alzheimer's diseases due to its misfolding [59]. Previous works demonstrated that Cu^{2+} could destabilize Aβ, promote protein oligomerization, and stabilize the Aβ oligomer [60,61]. Cu^{2+} enhances the stability of the Aβ oligomer by increasing the peptide–peptide binding forces [61]. It was further suggested that Cu^{2+} could bridge the peptides in the oligomers and form a Aβ–Cu–Aβ–Cu–··· structure by binding to the His residues from the two peptides, and thereby stabilize the Aβ oligomer. Based on the previous results, we herein make a hypothesis that Cu^{2+} could bridge monomeric PrP units in the PrP oligomer and form a PrP–Cu–PrP–Cu–··· structure. Nevertheless, further theoretically modeling and experimental studies are required to confirm this hypothesis.

Based on our results, the mechanism by which Cu^{2+}-binding promotes the oligomerization of PrP^C in prion diseases could be described as follows: Cu^{2+} binds to PrP^C and then induces significant conformation changes of PrP^C, which decreases the conformational stability of PrP^C, and thus facilitates the oligomerization of PrP^C. The formed PrP^O oligomers possess significant neurotoxicity. In addition, the presence of Cu^{2+} increases the stability of PrP^O. As reported previously, the central nervous system has high level of copper, and Cu^{2+} could increase the risk of neurodegenerative disorders, including prion diseases [11,12,62]. The present study demonstrated that Cu^{2+}-binding promotes the oligomerization of $HuPrP^C$ more significantly than that of $RaPrP^C$. Our results indicated that $HuPrP^C$ is much more susceptible to Cu^{2+} than $RaPrP^C$, which might make significant contribution to the conformational conversion of $HuPrP^C$ and the pathogenic process of human prion diseases. On the other hand, as one of the few species resistant to TSE diseases, rabbits are not infected by PrP^{Sc} under regular conditions [24], suggesting that the TSE-resistance of rabbits is highly associated with the crucial factors that significantly regulate the unique oligomerization process of $RaPrP^C$. Our results showed that $RaPrP^C$ possesses a low susceptibility to Cu^{2+} when compared with $HuPrP^C$. The low susceptibility of $RaPrP^C$ to Cu^{2+} may contribute to the difficulty of conformational conversion from normal cellular form to pathogenic scrapie isoform, which potentially weakens the risk of Cu^{2+}-induced TSE diseases.

In summary, Cu^{2+} plays vital roles in pathogenic prion diseases via participating in the oligomerization process of the PrP. Our results demonstrated that Cu^{2+} binds to both $HuPrP^C$ and $RaPrP^C$ with moderate affinity. Cu^{2+}-binding induces significant conformational change of PrP^C, and decreases the conformational stability of PrP^C, thereby promoting the conversion of α-helix-rich PrP^C into β-sheet-rich form and thus facilitating the oligomerization of PrP^C. Moreover, our results also indicated that $RaPrP^C$ has a lower susceptibility to Cu^{2+} than $HuPrP^C$. The unique properties of $RaPrP^C$ mostly contribute to the TSE-resistance of rabbits. This work is of great benefit to the mechanistic understanding of Cu^{2+}-binding-induced conformational conversion of PrP, and sheds light on the resistance of rabbits to prion diseases.

Supplementary Data

Supplementary data is available at *ABBS* online.

Funding

This work was supported by the grants from the National Natural Science Foundation of China (Nos. 31170717, 31470034, and 31270777).

References

1. Prusiner SB. Prions. *Proc Natl Acad Sci USA* 1998, 95: 13363–13383.
2. Brown DR, Qin K, Herms JW, Madlung A, Manson J, Strome R, Fraser PE, *et al*. The cellular prion protein binds copper *in vivo*. *Nature* 1997, 390: 684–687.
3. Prusiner SB. Novel proteinaceous infectious particles cause scrapie. *Science* 1982, 216: 136–144.
4. Caughey BW, Dong A, Bhat KS, Ernst D, Hayes SF, Caughey WS. Secondary structure analysis of the scrapie-associated protein PrP 27-30 in water by infrared spectroscopy. *Biochemistry* 1991, 30: 7672–7680.
5. Pan KM, Baldwin M, Nguyen J, Gasset M, Serban A, Groth D, Mehlhorn I, *et al*. Conversion of alpha-helices into beta-sheets features in the formation of the scrapie prion proteins. *Proc Natl Acad Sci USA* 1993, 90: 10962–10966.
6. Simoneau S, Rezaei H, Sales N, Kaiser-Schulz G, Lefebvre-Roque M, Vidal C, Fournier JG, *et al*. *In vitro* and *in vivo* neurotoxicity of prion protein oligomers. *PLoS Pathog* 2007, 3: e125.
7. Silveira JR, Raymond GJ, Hughson AG, Race RE, Sim VL, Hayes SF, Caughey B. The most infectious prion protein particles. *Nature* 2005, 437: 257–261.
8. Huang L, Jin R, Li J, Luo K, Huang T, Wu D, Wang W, *et al*. Macromolecular crowding converts the human recombinant PrPC to the soluble neurotoxic beta-oligomers. *FASEB J* 2010, 24: 3536–3543.
9. Madsen E, Gitlin JD. Copper and iron disorders of the brain. *Annu Rev Neurosci* 2007, 30: 317–337.
10. Skjorringe T, Moller LB, Moos T. Impairment of interrelated iron- and copper homeostatic mechanisms in brain contributes to the pathogenesis of neurodegenerative disorders. *Front Pharmacol* 2012, 3: 169.

11. Gaggelli E, Kozlowski H, Valensin D, Valensin G. Copper homeostasis and neurodegenerative disorders (Alzheimer's, prion, and Parkinson's diseases and amyotrophic lateral sclerosis). *Chem Rev* 2006, 106: 1995–2044.
12. Hung YH, Bush AI, Cherny RA. Copper in the brain and Alzheimer's disease. *J Biol Inorg Chem* 2010, 15: 61–76.
13. Brewer GJ. Copper excess, zinc deficiency, and cognition loss in Alzheimer's disease. *Biofactors* 2012, 38: 107–113.
14. Desai V, Kaler SG. Role of copper in human neurological disorders. *Am J Clin Nutr* 2008, 88: 855S–858S.
15. Brown DR. Copper and prion disease. *Brain Res Bull* 2001, 55: 165–173.
16. Mitteregger G, Korte S, Shakarami M, Herms J, Kretzschmar HA. Role of copper and manganese in prion disease progression. *Brain Res* 2009, 1292: 155–164.
17. Siggs OM, Cruite JT, Du X, Rutschmann S, Masliah E, Beutler B, Oldstone MB. Disruption of copper homeostasis due to a mutation of Atp7a delays the onset of prion disease. *Proc Natl Acad Sci USA* 2012, 109: 13733–13738.
18. Thackray AM, Knight R, Haswell SJ, Bujdoso R, Brown DR. Metal imbalance and compromised antioxidant function are early changes in prion disease. *Biochem J* 2002, 362: 253–258.
19. Qin K, Yang DS, Yang Y, Chishti MA, Meng LJ, Kretzschmar HA, Yip CM, *et al*. Copper(II)-induced conformational changes and protease resistance in recombinant and cellular PrP. Effect of protein age and deamidation. *J Biol Chem* 2000, 275: 19121–19131.
20. Kuczius T, Buschmann A, Zhang W, Karch H, Becker K, Peters G, Groschup MH. Cellular prion protein acquires resistance to proteolytic degradation following copper ion binding. *Biol Chem* 2004, 385: 739–747.
21. Johnson CJ, Gilbert PU, Abrecht M, Baldwin KL, Russell RE, Pedersen JA, Aiken JM, *et al*. Low copper and high manganese levels in prion protein plaques. *Viruses* 2013, 5: 654–662.
22. Wu D, Zhang W, Luo Q, Luo K, Huang L, Wang W, Huang T, *et al*. Copper (II) promotes the formation of soluble neurotoxic PrP oligomers in acidic environment. *J Cell Biochem* 2010, 111: 627–633.
23. Requena JR, Groth D, Legname G, Stadtman ER, Prusiner SB, Levine RL. Copper-catalyzed oxidation of the recombinant SHa(29-231) prion protein. *Proc Natl Acad Sci USA* 2001, 98: 7170–7175.
24. Pauli G. Tissue safety in view of CJD and variant CJD. *Cell Tissue Bank* 2005, 6: 191–200.
25. Lansbury PT Jr. Structural neurology: are seeds at the root of neuronal degeneration? *Neuron* 1997, 19: 1151–1154.
26. Prusiner SB. Prions. *Sci Am* 1984, 251: 50–59.
27. Vorberg I, Groschup MH, Pfaff E, Priola SA. Multiple amino acid residues within the rabbit prion protein inhibit formation of its abnormal isoform. *J Virol* 2003, 77: 2003–2009.
28. Chianini F, Fernandez-Borges N, Vidal E, Gibbard L, Pintado B, de Castro J, Priola SA, *et al*. Rabbits are not resistant to prion infection. *Proc Natl Acad Sci USA* 2012, 109: 5080–5085.
29. Fernandez-Borges N, Chianini F, Erana H, Vidal E, Eaton SL, Pintado B, Finlayson J, *et al*. Naturally prion resistant mammals: a utopia? *Prion* 2012, 6: 425–429.
30. Yuan Z, Zhao D, Yang L. Decipher the mechanisms of rabbit's low susceptibility to prion infection. *Acta Biochim Biophys Sin (Shanghai)* 2013, 45: 899–903.
31. Zhou Z, Yan X, Pan K, Chen J, Xie ZS, Xiao GF, Yang FQ, *et al*. Fibril formation of the rabbit/human/bovine prion proteins. *Biophys J* 2011, 101: 1483–1492.
32. Yan X, Huang JJ, Zhou Z, Chen J, Liang Y. How does domain replacement affect fibril formation of the rabbit/human prion proteins. *PLoS ONE* 2014, 9: e113238.
33. Wen Y, Li J, Xiong M, Peng Y, Yao W, Hong J, Lin D. Solution structure and dynamics of the I214V mutant of the rabbit prion protein. *PLoS ONE* 2010, 5: e13273.
34. Wen Y, Li J, Yao W, Xiong M, Hong J, Peng Y, Xiao G, *et al*. Unique structural characteristics of the rabbit prion protein. *J Biol Chem* 2010, 285: 31682–31693.
35. Hasnain SS, Murphy LM, Strange RW, Grossmann JG, Clarke AR, Jackson GS, Collinge J. XAFS study of the high-affinity copper-binding site of human PrP(91-231) and its low-resolution structure in solution. *J Mol Biol* 2001, 311: 467–473.
36. Cui PX, Lian FL, Wang Y, Wen Y, Chu WS, Zhao HF, Zhang S, *et al*. 3D local structure around copper site of rabbit prion-related protein: quantitative determination by XANES spectroscopy combined with multiple-scattering calculations. *Radiat Phys Chem* 2014, 95: 69–72.
37. Bjelic S, Jelesarov I. A survey of the year 2007 literature on applications of isothermal titration calorimetry. *J Mol Recognit* 2008, 21: 289–312.
38. Viles JH. Metal ions and amyloid fiber formation in neurodegenerative diseases. Copper, zinc and iron in Alzheimer's, Parkinson's and prion diseases. *Coord Chem Rev* 2012, 256: 2271–2284.
39. Bertinato J, L'Abbe MR. Maintaining copper homeostasis: regulation of copper-trafficking proteins in response to copper deficiency or overload. *J Nutr Biochem* 2004, 15: 316–322.
40. Waggoner DJ, Bartnikas TB, Gitlin JD. The role of copper in neurodegenerative disease. *Neurobiol Dis* 1999, 6: 221–230.
41. Gasperini L, Meneghetti E, Pastore B, Benetti F, Legname G. Prion protein and copper cooperatively protect neurons by modulating NMDA receptor through S-nitrosylation. *Antioxid Redox Signal* 2015, 22: 772–784.
42. Bocharova OV, Breydo L, Salnikov VV, Baskakov IV. Copper(II) inhibits *in vitro* conversion of prion protein into amyloid fibrils. *Biochemistry* 2005, 44: 6776–6787.
43. Younan ND, Klewpatinond M, Davies P, Ruban AV, Brown DR, Viles JH. Copper(II)-induced secondary structure changes and reduced folding stability of the prion protein. *J Mol Biol* 2011, 410: 369–382.
44. Migliorini C, Sinicropi A, Kozlowski H, Luczkowski M, Valensin D. Copper-induced structural propensities of the amyloidogenic region of human prion protein. *J Biol Inorg Chem* 2014, 19: 635–645.
45. Kovacs GG, Gelpi E, Strobel T, Ricken G, Nyengaard JR, Bernheimer H, Budka H. Involvement of the endosomal-lysosomal system correlates with regional pathology in Creutzfeldt-Jakob disease. *J Neuropathol Exp Neurol* 2007, 66: 628–636.
46. Thompsett AR, Abdelraheim SR, Daniels M, Brown DR. High affinity binding between copper and full-length prion protein identified by two different techniques. *J Biol Chem* 2005, 280: 42750–42758.
47. Salmona M, Malesani P, De Gioia L, Gorla S, Bruschi M, Molinari A, Della Vedova F, *et al*. Molecular determinants of the physicochemical properties of a critical prion protein region comprising residues 106–126. *Biochem J* 1999, 342 (Pt 1): 207–214.
48. Jobling MF, Stewart LR, White AR, McLean C, Friedhuber A, Maher F, Beyreuther K, *et al*. The hydrophobic core sequence modulates the neurotoxic and secondary structure properties of the prion peptide 106–126. *J Neurochem* 1999, 73: 1557–1565.
49. Walsh P, Simonetti K, Sharpe S. Core structure of amyloid fibrils formed by residues 106–126 of the human prion protein. *Structure* 2009, 17: 417–426.
50. Jones CE, Abdelraheim SR, Brown DR, Viles JH. Preferential Cu2+ coordination by His96 and His111 induces beta-sheet formation in the unstructured amyloidogenic region of the prion protein. *J Biol Chem* 2004, 279: 32018–32027.
51. Cliff MJ, Ladbury JE. A survey of the year 2002 literature on applications of isothermal titration calorimetry. *J Mol Recognit* 2003, 16: 383–391.
52. Quaglio E, Chiesa R, Harris DA. Copper converts the cellular prion protein into a protease-resistant species that is distinct from the scrapie isoform. *J Biol Chem* 2001, 276: 11432–11438.
53. Baskakov IV, Aagaard C, Mehlhorn I, Wille H, Groth D, Baldwin MA, Prusiner SB, *et al*. Self-assembly of recombinant prion protein of 106 residues. *Biochemistry* 2000, 39: 2792–2804.
54. Baskakov IV, Legname G, Prusiner SB, Cohen FE. Folding of prion protein to its native alpha-helical conformation is under kinetic control. *J Biol Chem* 2001, 276: 19687–19690.
55. Riesner D, Kellings K, Post K, Wille H, Serban H, Groth D, Baldwin MA, *et al*. Disruption of prion rods generates 10-nm spherical particles having high alpha-helical content and lacking scrapie infectivity. *J Virol* 1996, 70: 1714–1722.
56. Tzaban S, Friedlander G, Schonberger O, Horonchik L, Yedidia Y, Shaked G, Gabizon R, *et al*. Protease-sensitive scrapie prion protein in aggregates of heterogeneous sizes. *Biochemistry* 2002, 41: 12868–12875.

57. Ladner CL, Wishart DS. Resolution-enhanced native acidic gel electrophoresis: a method for resolving, sizing, and quantifying prion protein oligomers. *Anal Biochem* 2012, 426: 54–62.
58. Apetri AC, Surewicz WK. Atypical effect of salts on the thermodynamic stability of human prion protein. *J Biol Chem* 2003, 278: 22187–22192.
59. Ballard C, Gauthier S, Corbett A, Brayne C, Aarsland D, Jones E. Alzheimer's disease. *Lancet* 2011, 377: 1019–1031.
60. Han D, Wang H, Yang P. Molecular modeling of zinc and copper binding with Alzheimer's amyloid beta-peptide. *Biometals* 2008, 21: 189–196.
61. Hane F, Tran G, Attwood SJ, Leonenko Z. Cu(2+) affects amyloid-beta (1–42) aggregation by increasing peptide-peptide binding forces. *PLoS ONE* 2013, 8: e59005.
62. Sigurdsson EM, Brown DR, Alim MA, Scholtzova H, Carp R, Meeker HC, Prelli F, *et al*. Copper chelation delays the onset of prion disease. *J Biol Chem* 2003, 278: 46199–46202.